Linearized Downconverting Microwave Photonic Link Using Dual-Wavelength Phase Modulation and Optical Filtering

Bryan M. Haas, *Member, IEEE*, and T. E. Murphy, *Senior Member, IEEE*

Laboratory for Physical Sciences and Department of Electrical and Computer Engineering, University of Maryland, College Park, MD 20742 USA

DOI: 10.1109/JPHOT.2010.2095414
1943-0655/$26.00 ©2010 IEEE

Manuscript received November 17, 2010; accepted November 18, 2010. Date of publication November 23, 2010; date of current version January 24, 2011. Corresponding author: T. E. Murphy (e-mail: tem@umd.edu).

Abstract: We describe a technique transmitting K-band microwave signals over an optical channel using electrooptic phase modulation at the transmitter followed by series phase modulation and bandpass filtering in the receiver to downconvert the transmitted signal to an intermediate frequency (IF). Unlike other downconversion methods, the method does not require a microwave mixer, high-speed optical photoreceivers, optically stabilized local oscillator, or active bias control at either phase modulator. We further show that the link can be linearized by using two wavelengths launched along orthogonal axes of a single lithium niobate phase modulator at the transmitter. We successfully demonstrate linearized downconversion of a 20-GHz microwave signal to a 250-MHz IF. The linearization method results in a 14-dB improvement in the spurious-free dynamic range compared with the nonlinearized case.

Index Terms: Submillimeter wave radio communication, microwave communication, optical fiber communication, electrooptic modulation, heterodyning.

1. Introduction

One of the problems faced by RF engineers is how to efficiently transfer a high frequency microwave signal between the antenna and receiver (or transmitter) when they are separated by some significant distance. There is a large body of literature discussing the merits and handicaps of using fiber optic links to perform this function, usually using intensity modulated links with direct detection (IMDD) links [1]–[4].

A growing number of efforts have recently focused on phase-modulated links as another alternative because of the highly linear modulation it provides and simpler modulator/transmitter [5]–[8]. Several recent efforts at developing linear, or linearized, optical receivers are bearing fruit, although they are limited in bandwidth [9], [10] or require additional digital processing [11].

Another problem is how to recover the high-frequency signal in a way that it can be digitized with high resolution. This usually requires the signal to be downconverted to an intermediate frequency (IF), often in the VHF band, that is better suited to high-performance analog-to-digital conversion. A fiber optic link that does not downconvert the signal must use an electronic mixer to accomplish this, either before or after the link. If the mixer is placed after the link, the photodetectors and mixers must have enough bandwidth to accommodate the full-spectrum microwave signal, which can add significant cost and complexity.

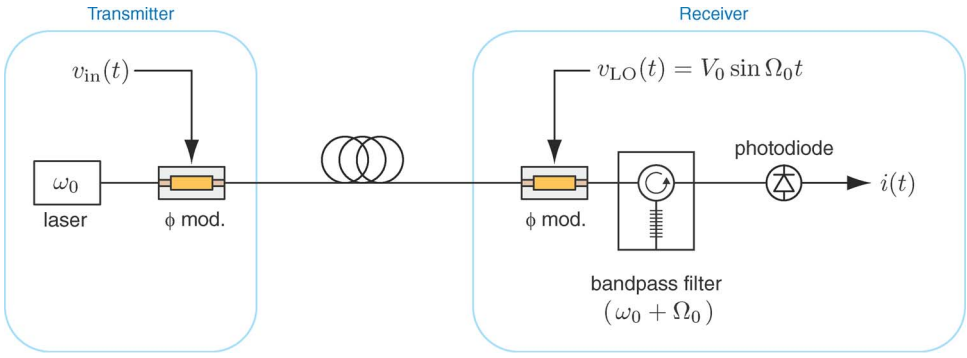

Fig. 1. Simplified diagram of downconversion scheme based on cascaded phase modulation followed by optical bandpass filtering.

We describe here a new method that instead uses electrooptic mixing in a local oscillator (LO)-driven phase modulator. The method presented here is limited in that the optical filter must be able to spectrally separate one optical sideband from its neighbors, placing a practical lower frequency limit at a few gigahertz with conventional filter technology. Thus, this link works most effectively at higher gigahertz frequencies, where it becomes easier to spectrally filter the sideband. This technique is uniquely suited for burgeoning applications that utilize the K and Ka bands (18–40 GHz). Furthermore, we demonstrate that the system can be linearized by using two wavelengths, each launched along orthogonal polarization states of the phase modulator.

2. Downconversion Theory

Fig. 1 is a simplified block diagram of the downconversion scheme reported here. At the transmitter, a continuous-wave (CW) laser is phase-modulated by a microwave signal and transmitted over fiber to the receiver. In the receiver, the signal enters a second phase modulator that is driven by a strong microwave LO. The optical bandpass filter is tuned to the first upper sideband of the modulated optical signal.

We assume that the first phase modulator is driven by a two-tone microwave signal

$$v_{in}(t) = V_1 \sin\Omega_1 t + V_2 \sin\Omega_2 t \tag{1}$$

so that the emerging optical signal is given by

$$u(t) = \sqrt{P_0}\, e^{j\omega_0 t} e^{jm_1 \sin\Omega_1 t} e^{jm_2 \sin\Omega_2 t} \tag{2}$$

where P_0 is the optical power, ω_0 is the optical frequency, and m_i is the modulation amplitude (in radians) of the ith frequency tone

$$m_i \equiv \pi \frac{V_i}{V_\pi}. \tag{3}$$

Fig. 2(a) depicts the optical spectrum of the phase-modulated signal after leaving the transmitter, showing the optical carrier and upper sideband with two tones.

When the signal reaches the receiver, it is re-modulated with a second phase modulator driven by a strong microwave LO

$$v_{LO}(t) = V_0 \sin\Omega_0 t \tag{4}$$

where the LO frequency Ω_0 is tuned in the vicinity of the signal frequencies Ω_1 and Ω_2, with the aim of producing downconverted mixing products at $(\Omega_1 - \Omega_0)$ and $(\Omega_2 - \Omega_0)$.

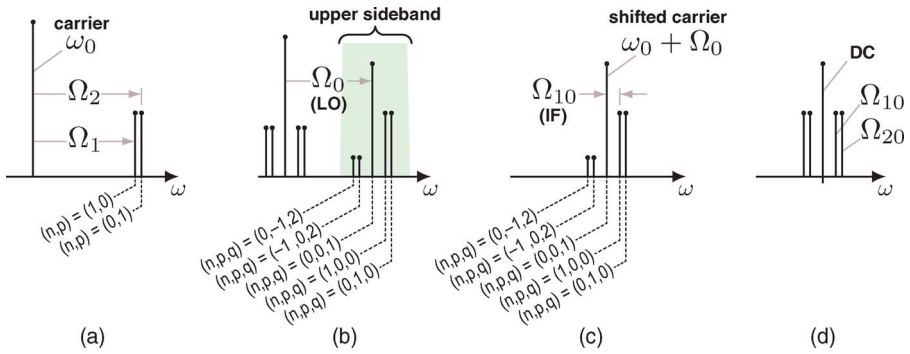

Fig. 2. (a) Optical spectrum after the first phase modulator showing the carrier (ω_0) and the upper sidebands created by the two-tone phase modulation. (b) Optical spectrum after the second phase modulator and (c) following the bandpass filter. (d) Electrical spectrum of the resulting photocurrent $i(t)$ showing the two downconverted frequencies.

The optical field after the second phase modulator is then given by

$$u(t) = \sqrt{P_0}e^{j\omega_0 t}e^{jm_1\sin\Omega_1 t}e^{jm_2\sin\Omega_2 t}e^{jm_0\sin\Omega_0 t} \tag{5}$$

where m_0 is the modulation depth of the LO, which is defined analogously to (3). Fig. 2(b) shows the optical spectrum after LO modulation.

Applying the Jacobi–Anger expansion to all three of the exponentials in (5) gives

$$u(t) = \sqrt{P_0}e^{j\omega_0 t}\sum_{n,p,q}\left[J_n(m_1)J_p(m_2)J_q(m_0)e^{j(n\Omega_1+p\Omega_2+q\Omega_0)t}\right] \tag{6}$$

where all three summations extend from $-\infty$ to $+\infty$.

The signal then passes through an optical bandpass filter that is tuned to the upper modulation sideband, resulting in the spectrum indicated schematically in Fig. 2(c). We make the assumption that the filter is an ideal optical bandpass filter that transmits only those terms from (6) for which $n+p+q=1$. This allows us to set $q=1-n-p$ and eliminate the summation over q

$$u(t) = \sqrt{P_0}e^{j(\omega_0+\Omega_0)t}\sum_{n,p}\left[J_n(m_1)J_p(m_2)J_{1-n-p}(m_0)e^{j(n\Omega_{10}+p\Omega_{20})t}\right] \tag{7}$$

where we have introduced the downconverted IF frequencies

$$\Omega_{10} \equiv \Omega_1 - \Omega_0, \quad \Omega_{20} \equiv \Omega_2 - \Omega_0. \tag{8}$$

After the bandpass filter, the signal is detected in a square-law photodetector, resulting in a photocurrent

$$i(t) = \mathcal{R}|u(t)|^2 \tag{9}$$

where $\mathcal{R}$ is the responsivity of the photodiode. Substituting (7) into (9) gives

$$i(t) = \mathcal{R}P_0\sum_{n,p,r,s}\left[J_n(m_1)J_p(m_2)J_r(m_1)J_s(m_2)\times J_{1-n-p}(m_0)J_{1-r-s}(m_0)e^{j[(n-r)\Omega_{10}+(p-s)\Omega_{20}]t}\right]. \tag{10}$$

When the input signals are small, we may expand the product $J_n(m_1)J_p(m_2)J_r(m_1)J_s(m_2)$ in a power series, retaining only the terms up to first order in m_1 or m_2. One need only consider those

terms in the quadruple summation for which $|n| + |p| + |r| + |s| = 0$ or 1. After some simplification, this yields

$$i(t) = \mathcal{R}P_0\Big\{J_1^2(m_0) \tag{11}$$

$$+ J_1(m_0)[J_0(m_0) - J_2(m_0)]m_1\cos\Omega_{10}t \tag{12}$$

$$+ J_1(m_0)[J_0(m_0) - J_2(m_0)]m_2\cos\Omega_{20}t\Big\}. \tag{13}$$

To first order, the received signal comprises a DC photocurrent (11) and downconverted signals at the IF frequencies Ω_{10} and Ω_{20}, as indicated in Fig. 2(d).

If the photodiode drives an output impedance of Z_{out}, then the downconverted power at Ω_{10} is

$$P_{\text{out}} = \frac{1}{2}\{\mathcal{R}P_0J_1(m_0)[J_0(m_0) - J_2(m_0)]m_1\}^2Z_{\text{out}}. \tag{14}$$

If the phase modulator has an input impedance of Z_{in}, then the input microwave power at Ω_1 is

$$P_{\text{in}} = \frac{1}{2}\frac{V_1^2}{Z_{\text{in}}} = \frac{V_\pi^2}{2\pi^2Z_{\text{in}}}m_1^2. \tag{15}$$

Taking the ratio of (14) to (15), the net RF downconversion gain (or loss) is found to be

$$G = (2J_1(m_0)[J_0(m_0) - J_2(m_0)])^2G_0 \tag{16}$$

where G_0 is defined as

$$G_0 \equiv \left(\frac{\pi\mathcal{R}P_0}{2V_\pi}\right)^2Z_{\text{out}}Z_{\text{in}} \tag{17}$$

which represents the gain of a nondownconverting link employing a quadrature-biased Mach–Zehnder intensity modulator with direct detection.

For a fixed optical power P_0, the downconversion gain G can be maximized by choosing the LO modulation depth of

$$m_0^{(\text{opt})} \simeq 0.9116, \quad V_0 = 0.2902V_\pi. \tag{18}$$

The optimal gain achieved under these conditions is

$$G^{(\text{opt})} = (0.3352)G_0. \tag{19}$$

Earlier demonstrations of electrooptic downconversion have used, among other techniques, a pair of cascaded quadrature-biased Mach–Zehnder modulators, one of which is driven by a strong LO [12]–[18]. This configuration exhibits a downconversion gain of [19], [20]

$$G = J_1^2(m_0)G_0 \tag{20}$$

which achieves a maximum value of

$$G^{(\text{opt})} = (0.3384)G_0 \tag{21}$$

when the LO modulation depth is chosen to be $m_0 = 1.8412$. Upconversion and downconversion has also been implemented using electrooptic phase modulation, together with chromatic dispersion in a long fiber span to convert the phase-modulated signal to an intensity modulated signal at the output [21], [22].

TABLE 1

Expansion coefficients Φ_{np} describing the DC, fundamental, third-order, and fifth-order intermodulation distortion products that contribute to the photocurrent $i(t)$ in (22)–(27). The right-most two columns tabulate the corresponding output frequencies and the power-law dependence on m_1 and m_2

$\Phi_{00}(x)$	$J_1^2(x)$	0 (DC)	1
$\Phi_{10}(x)$	$J_1(x)J_0(x) - J_2(x)J_1(x)$	Ω_{10}, Ω_{20}	$m_1,\ m_2$
$\Phi_{21}(x)$	$-\frac{1}{8}[4J_1(x)J_0(x) - 3J_2(x)J_1(x) + J_3(x)J_2(x)]$	$(2\Omega_{10} - \Omega_{20}), (2\Omega_{20} - \Omega_{10})$	$m_1^2 m_2,\ m_2^2 m_1$
$\Phi_{23}(x)$	$\frac{1}{64}[15J_1(x)J_0(x) - 11J_2(x)J_1(x) + 5J_3(x)J_2(x) - J_4(x)J_3(x)]$	$(2\Omega_{10} - \Omega_{20}), (2\Omega_{20} - \Omega_{10})$	$m_1^2 m_2^3,\ m_2^2 m_1^3$
$\Phi_{41}(x)$	$\frac{1}{48}[7J_1(x)J_0(x) - 5J_2(x)J_1(x) + 2J_3(x)J_2(x)]$	$(2\Omega_{10} - \Omega_{20}), (2\Omega_{20} - \Omega_{10})$	$m_1^4 m_2,\ m_2^4 m_1$
$\Phi_{32}(x)$	$\frac{1}{192}[15J_1(x)J_0(x) - 11J_2(x)J_1(x) + 5J_3(x)J_2(x) - J_4(x)J_3(x)]$	$(3\Omega_{10} - 2\Omega_{20}), (3\Omega_{20} - 2\Omega_{10})$	$m_1^3 m_2^2,\ m_2^3 m_1^2$

The scheme described here gives a net RF downconversion gain comparable with what was achieved in earlier systems but requires only phase modulation and bandpass filtering.

3. Intermodulation Distortion

Extending the expansion of (10) to higher order reveals additional in-band distortion products that are absent from the input. Retaining terms in the expansion up to fifth order in m_i, one obtains intermodulation products at the frequencies $(2\Omega_{10} - \Omega_{20})$, $(2\Omega_{20} - \Omega_{10})$, $(3\Omega_{10} - 2\Omega_{20})$, and $(3\Omega_{20} - 2\Omega_{10})$. After some algebraic simplification, the resulting photocurrent, to fifth order, is found to be

$$
\begin{aligned}
i(t) = \mathcal{R}P_0[&\Phi_{00}(m_0) && (22)\\
&+ \Phi_{10}(m_0)(m_1\cos\Omega_{10}t + m_2\cos\Omega_{20}t) && (23)\\
&+ \Phi_{21}(m_0)m_1^2 m_2\cos(2\Omega_{10} - \Omega_{20})t && (24)\\
&+ \Phi_{23}(m_0)m_1^2 m_2^3\cos(2\Omega_{10} - \Omega_{20})t && (25)\\
&+ \Phi_{41}(m_0)m_1^4 m_2\cos(2\Omega_{10} - \Omega_{20})t && (26)\\
&+ \Phi_{32}(m_0)m_1^3 m_2^2\cos(3\Omega_{10} - 2\Omega_{20})t] && (27)\\
&+ \text{IMD terms at } (2\Omega_{20} - \Omega_{10}) \text{ and } (3\Omega_{20} - 2\Omega_{10})
\end{aligned}
$$

where the expansion coefficients $\Phi_{np}(m_0)$ are given in Table 1. Note that out-of-band harmonics and higher order corrections to the DC and fundamental terms are not included in (22)–(27).

The third-order intercept point is found by equating the extrapolated third-order distortion amplitude with the extrapolated fundamental amplitude, assuming both input tones have the same power $(m_1 = m_2 \equiv m)$. This gives

$$
m^2 = \left|\frac{\Phi_{10}(m_0)}{\Phi_{21}(m_0)}\right| = \left|\frac{8(J_1J_0 - J_2J_1)}{3J_2J_1 - J_3J_2 - 4J_1J_0}\right| \tag{28}
$$

or, in terms of the input microwave power (15), the input-referenced intercept point is

$$
P_{\text{IIP3}} = \frac{V_\pi^2}{2\pi^2 Z_{\text{in}}}\left|\frac{\Phi_{10}(m_0)}{\Phi_{21}(m_0)}\right|. \tag{29}
$$

4. Linearization

The linearization technique used here exploits the fact that the electrooptic coefficient of $LiNbO_3$ is different for the z (TM) and x (TE) polarization states. This effectively causes a single modulator to

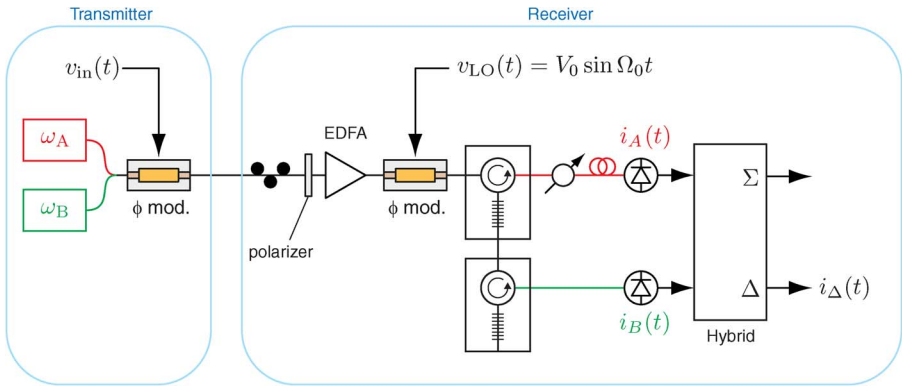

Fig. 3. Diagram of two-wavelength, two-polarization system scheme for achieving linearized downconversion.

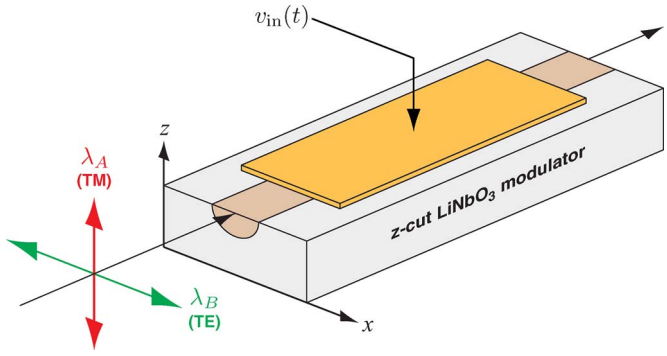

Fig. 4. Two optical wavelengths are polarization-multiplexed and launched along orthogonal axes of a $LiNbO_3$ modulator. Because of anisotropy in the electrooptic coefficients, the *z*-polarized wavelength is phase-modulated more strongly than the *x*-polarized wavelength.

act as two modulators with different transfer functions that can be set in opposition to suppress a single order of distortion [23]–[27]. To facilitate separation of the orthogonally polarized signals, we use a different wavelength for each polarization [9], and each is separately recovered with the filtered sideband method and the detected currents combined.

Fig. 3 is a diagram of the linearized downconversion system. At the transmitter, two optical sources are polarization-multiplexed and launched along the orthogonal axes of the phase modulator, as detailed in Fig. 4.

The optical field entering the first phase modulator can be represented as

$$\mathbf{u}(t) = \hat{\mathbf{z}}\sqrt{P_A}e^{j\omega_A t} + \hat{\mathbf{x}}\sqrt{P_B}e^{j\omega_B t} \tag{30}$$

where P_A, P_B, ω_A, and ω_B are the powers and optical frequencies of the two lasers.

As before, we assume that the modulator is driven by a two-tone microwave signal. The vector optical field emerging from the first phase modulator is given by

$$\mathbf{u}(t) = \hat{\mathbf{z}}\sqrt{P_A}e^{j\omega_A t}e^{jm_1\sin\Omega_1 t}e^{jm_2\sin\Omega_2 t} + \hat{\mathbf{x}}\sqrt{P_B}e^{j\omega_B t}e^{j\gamma m_1\sin\Omega_1 t}e^{j\gamma m_2\sin\Omega_2 t} \tag{31}$$

where m_i represents the modulation depth for the $\hat{\mathbf{z}}$, or TM, polarization state, i.e.,

$$m_1 \equiv \pi\frac{V_1}{V_\pi^{(\rm TM)}}, \quad m_2 \equiv \pi\frac{V_2}{V_\pi^{(\rm TM)}}. \tag{32}$$

The $\hat{x}$, or TE, polarization state is phase modulated less efficiently than the TM polarization. The ratio γ relates the modulation depths for TE and TM polarizations

$$\gamma \equiv \frac{V_\pi^{(\mathrm{TM})}}{V_\pi^{(\mathrm{TE})}}. \tag{33}$$

In lithium-niobate and most poled electrooptic polymers, we find $\gamma \simeq 1/3$.

When the signal reaches the receiver, it is projected onto a fixed linear polarization axis and amplified by a polarizing erbium-doped fiber amplifier (EDFA). The scalar field emerging from the amplifier can be expressed as

$$u(t) = \sqrt{P'_A}e^{j\omega_A t}e^{jm_1\sin\Omega_1 t}e^{jm_2\sin\Omega_2 t} + \sqrt{P'_B}e^{j\omega_B t}e^{j\gamma m_1\sin\Omega_1 t}e^{j\gamma m_2\sin\Omega_2 t} \tag{34}$$

where P'_A and P'_B represent the amplified output powers of the two optical wavelengths after the polarizing EDFA. The relative strengths of P'_A and P'_B can be adjusted using a polarization controller prior to the receiver.

Following amplification, the two wavelengths are remodulated, as before, with a strong microwave LO. After the local phase modulator, the optical field is given by

$$u(t) = \sqrt{P'_A}e^{j\omega_A t}e^{jm_1\sin\Omega_1 t}e^{jm_2\sin\Omega_2 t}e^{jm_0\sin\Omega_0 t} + \sqrt{P'_B}e^{j\omega_B t}e^{j\gamma m_1\sin\Omega_1 t}e^{j\gamma m_2\sin\Omega_2 t}e^{jm_0\sin\Omega_0 t}. \tag{35}$$

The polarizing EDFA ensures that the two wavelengths are co-polarized in the receiver so that they are modulated by the same amount in the local phase modulator.

Using a pair of bandpass filters, the upper sidebands of the two optical waves are spectrally isolated and detected in two separate photoreceivers. Applying the results derived earlier, the photocurrents in the two detectors are found to be

$$\begin{aligned} i_A(t) = \mathcal{R}P'_A[&\Phi_{00}(m_0) + \Phi_{10}(m_0)(m_1\cos\Omega_{10}t + m_2\cos\Omega_{20}t) \\ &+ \Phi_{21}(m_0)m_1^2m_2\cos(2\Omega_{10} - \Omega_{20})t + \Phi_{23}(m_0)m_1^2m_2^3\cos(2\Omega_{20} - \Omega_{10})t \\ &+\Phi_{41}(m_0)m_1^4m_2\cos(2\Omega_{10} - \Omega_{20})t + \Phi_{32}(m_0)m_1^3m_2^2\cos(3\Omega_{10} - 2\Omega_{20})t] \\ &+ \text{terms at } (2\Omega_{20} - \Omega_{10}) \text{ and } (3\Omega_{20} - 2\Omega_{10}) \end{aligned} \tag{36}$$

$$\begin{aligned} i_B(t) = \mathcal{R}P'_B[&\Phi_{00}(m_0) + \Phi_{10}(m_0)(\gamma m_1\cos\Omega_{10}t + \gamma m_2\cos\Omega_{20}t) \\ &+ \Phi_{21}(m_0)\gamma^3m_1^2m_2\cos(2\Omega_{10} - \Omega_{20})t + \Phi_{23}(m_0)\gamma^5m_1^2m_2^3\cos(2\Omega_{20} - \Omega_{10})t \\ &+\Phi_{41}(m_0)\gamma^5m_1^4m_2\cos(2\Omega_{10} - \Omega_{20})t + \Phi_{32}(m_0)\gamma^5m_1^3m_2^2\cos(3\Omega_{10} - 2\Omega_{20})t] \\ &+ \text{terms at } (2\Omega_{20} - \Omega_{10}) \text{ and } (3\Omega_{20} - 2\Omega_{10}). \end{aligned} \tag{37}$$

The two photocurrents are subtracted using a 180° hybrid coupler, which produces an output photocurrent of

$$i_\Delta(t) = \frac{1}{\sqrt{2}}[i_A(t) - i_B(t)]. \tag{38}$$

We note that the factor of $1/\sqrt{2}$ could be eliminated by using a balanced photodiode pair instead of a microwave hybrid coupler.

When (36) and (37) are subtracted, the third-order intermodulation terms proportional to $m_1^2m_2$ will cancel, provided the powers are chosen to satisfy the following condition:

$$P'_A = \gamma^3 P'_B. \tag{39}$$

This linearization condition can be reexpressed as

$$P'_A = \frac{\gamma^3}{1+\gamma^3} P_0, \quad P'_B = \frac{1}{1+\gamma^3} P_0 \tag{40}$$

where $P_0 \equiv P'_A + P'_B$ is the total optical power after the EDFA.

Under this condition, the output photocurrent is given by

$$\begin{aligned} i_\Delta(t) = -\frac{\mathcal{R}P_0}{\sqrt{2}(1+\gamma^3)} &[(1-\gamma^3)\Phi_{00}(m_0) + \gamma(1-\gamma^2)\Phi_{10}(m_0)(m_1 \cos\Omega_{10} t + m_2 \cos\Omega_{20} t) \\ &- \gamma(1-\gamma^2)\Phi_{23}(m_0) m_1^2 m_2^3 \cos(2\Omega_{10} - \Omega_{20})t - \gamma(1-\gamma^2)\Phi_{41}(m_0) m_1^4 m_2 \\ &\times \cos(2\Omega_{10} - \Omega_{20})t - \gamma(1-\gamma^2)\Phi_{32}(m_0) m_1^3 m_2^2 \cos(3\Omega_{10} - 2\Omega_{20})t \\ &+ \text{terms at } (2\Omega_{20} - \Omega_{10}) \text{ and } (3\Omega_{20} - 2\Omega_{10}) \end{aligned} \tag{41}$$

in which the third-order intermodulation terms are seen to be absent, and the system is limited instead by fifth-order intermodulation distortion.

The net RF gain (including downconversion) of the linearized link is given by

$$G = \frac{1}{2}\left[\frac{\gamma(1-\gamma^2)}{(1+\gamma^3)} 2\Phi_{10}(m_0)\right]^2 \left(\frac{\pi \mathcal{R} P_0}{2V_\pi}\right)^2 Z_{\text{out}} Z_{\text{in}}. \tag{42}$$

Comparing this gain with that of the single-polarization, single-wavelength case (16), we find that (assuming the same m_0) the RF gain is reduced by a factor of

$$\frac{1}{2}\left[\frac{\gamma(1-\gamma^2)}{(1+\gamma^3)}\right]^2$$

although the factor of 1/2 could be eliminated by using a balanced photodiode instead of a hybrid coupler.

If the two input amplitudes are equal ($m_1 = m_2 \equiv m$), the terms proportional to $m_1^2 m_2^3$ and $m_1^4 m_2$ can be combined into a single term proportional to $[\Phi_{23}(m_0) + \Phi_{41}(m_0)]m^5$. This term is typically larger than the remaining IMD product at $(3\Omega_{20} - 2\Omega_{10})$. The fifth-order intercept point is found by equating the extrapolated amplitudes of the fundamental and dominant intermodulation products, which gives

$$m^4 = \left|\frac{\Phi_{10}(m_0)}{\Phi_{23}(m_0) + \Phi_{41}(m_0)}\right|. \tag{43}$$

The input-referenced intercept point is then calculated to be

$$P_{\text{IIP5}} = \frac{V_\pi^2}{2\pi^2 Z_{\text{in}}} \left|\frac{\Phi_{10}(m_0)}{\Phi_{23}(m_0) + \Phi_{41}(m_0)}\right|^{1/2}. \tag{44}$$

The degree to which the third-order intermodulation distortion can be suppressed depends on how accurately the two relative powers P'_A and P'_B can be adjusted and controlled. To quantify this dependence, we imagine that the two powers are adjusted with some arbitrary splitting ratio, which is denoted κ

$$P'_A = \kappa P_0 \quad P'_B = (1-\kappa)P_0. \tag{45}$$

As explained earlier, the third-order intermodulation products are eliminated by the choosing $\kappa = \gamma^3/(1+\gamma^3)$. We now consider a small deviation from this optimal condition

$$\kappa = \frac{\gamma^3}{1+\gamma^3} + \delta. \tag{46}$$

The degree of third-order suppression, relative to the nonlinearized case when $\kappa = 0$, is then calculated to be

$$\frac{P_{\mathrm{IMD3}}(\kappa)}{P_{\mathrm{IMD3}}(\kappa = 1)} = \delta^2(1-\gamma^3)^2. \tag{47}$$

The amount of suppression needed to achieve adequate linearization depends on the noise floor, which is in turn related to the electrical bandwidth of the receiver. For the measurements reported here, we were able to adjust and maintain δ to a precision of at least 0.001, which allowed us to achieve better than 60 dB suppression of the IMD3 products, relative to the nonlinearized case.

5. Experiment

Two external cavity tunable lasers were polarization multiplexed onto the slow (TM) and fast (TE) axes of the signal modulator's input polarization-maintaining (PM) fiber. The TE wavelength was launched onto the fast axis by means of a 90° PM splice. The signal modulator was a 5 cm long, 40 GHz, z-cut Ti-indiffused $LiNbO_3$ phase modulator. At a microwave frequency of 20 GHz, the half-wave voltage V_π was measured at to be 7.4 V for TM polarization and 20.5 V for the TE polarization, thus giving a ratio $\gamma = 0.361$. The phase modulator was driven with two equal-power microwave tones at 19.95 and 19.98 GHz.

The polarization isolation between the two wavelengths, measured at the output of the modulator, was $>$ 24 dB. Imperfect polarization or spectral isolation in the modulator or at the detectors does not preclude linearization, as long as the net modulation depth on each wavelength is different. Any crosstalk will effectively change the ratio γ, thereby changing received powers P'_A and P'_B needed for linearization according to (39) and changing the received gain and dynamic range.

The output of the modulator traveled through a length of single-mode fiber to a polarization controller and then into a single polarization EDFA with an 11-dB optical noise figure. The polarization controller was adjusted to ensure sufficient power from each wavelength entered the EDFA, and the single-polarization output from the EDFA was aligned along the TM axis of the LO modulator. This guarantees that both wavelengths experienced the same LO modulation depth.

The LO phase modulator was driven by a single 19.7-GHz tone with a microwave power of 18.1 dBm. The modulation depth was estimated to be $m_0 = 1.08$ by measuring the power in the first optical sidebands using an optical spectrum analyzer. The LO phase modulator was nominally identical to the signal modulator.

After both wavelengths were modulated with the LO, they were passed through a thermally stabilized fiber Bragg grating (FBG) with nominal 1 dB bandwidth of 30 GHz to separate out one of the wavelength's upper sidebands (first sideband of the signal and LO) on the reflective path. The remainder of the signal was transmitted to a second FBG that selected the other wavelength's upper sideband. This filtering both spectrally separated the two signals and enabled the IF down-conversion. A variable optical attenuator and variable time delay was inserted into one path to allow fine adjustment of the optical powers and to balance the group delays for the two paths.

Once separated, each signal was sent to a PIN photodetector. The photodetector outputs were combined in a 180° RF hybrid, with its output sent to a microwave spectrum analyzer via a bandpass filter and low-noise preamplifier to ensure that the link noise floor was visible above that of the spectrum analyzer. The optical powers were adjusted to achieve a DC photocurrent of 2.5 mA for the TM-only case. In the mixed polarization linearized case, the TE-polarized photocurrent was 2.5 mA, and the TM photocurrent was considerably smaller.

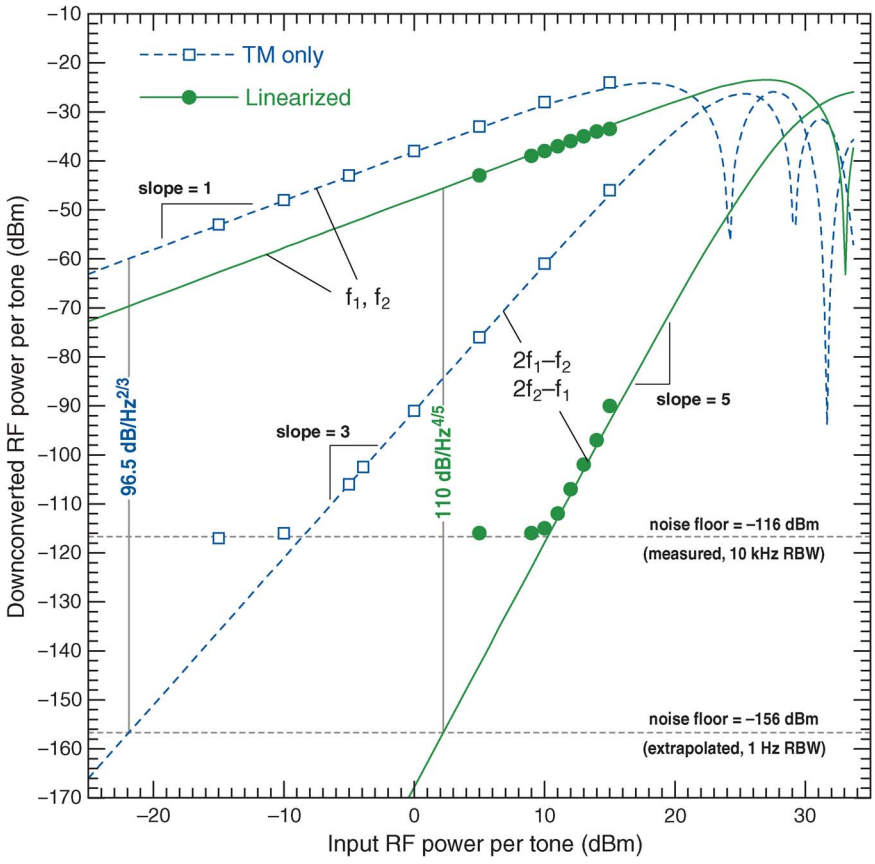

Fig. 5. Measured received versus input RF power for the TM-only (blue squares) and linearized (green circles). The lines indicate the results from theory. The input signal tones were at 19.95 GHz and 19.98 GHz with the downconverted IF tones at 250 MHz and 280 MHz. All measurements used a resolution bandwidth of 10 kHz.

TABLE 2

Predicted and measured link performance

predicted/measured	TM-only	Linearized
Gain	-37 / -37 dBm	-49 / -48 dBm
SFDR	97 / 96.5 dB/Hz$^{2/3}$	110.5 / 110 dB/Hz$^{4/5}$

The FBGs used in this experiment were far from ideal and only provided about 6.6 dB extinction at an offset of 20 GHz from the filter center. We estimate that this impairs the gain of the link by approximately 6.6 dB compared with an ideal bandpass filter with infinite out-of-band rejection. Despite this limitation, we were able to achieve downconversion and linearization.

6. Results and Discussion

Results from the two-tone testing are presented in Fig. 5 and summarized in Table 2. In all cases, the downconverted fundamental tones were measured at 250 MHz and 280 MHz, and the IMD products were measured at 220 MHz and 310 MHz. The curves in Fig. 5 indicate the calculated results, which agree well with the experimental measurements. The calculations include the 3-dB power loss from the hybrid combiner as well as a 6-dB loss from the parallel 50-Ω resistor in each photodiode.

Although the linearized SFDR achieved in this demonstration is not itself particularly impressive at 110 dB/Hz$^{4/5}$, the 13.5-dB improvement in dynamic range over the TM-only baseline is in agreement with theory. The TM-only Gain, NF, and SFDR also agree with the predicted values. Calculations show that in the shot limit and with the same V_π for the signal modulator, the linearized SFDR for the same received current improves to 122 dB/Hz$^{4/5}$. Calculations show that if the bandpass filters could provide a 20-dB rejection of the neighboring sidebands, the SFDR would further improve to 124 dB/Hz$^{4/5}$. It must also be recalled that the signal has already been downconverted from 20 GHz to a 250 MHz IF; conventional links generally require an additional electronic mixer, which can further compromise the SFDR.

The FBGs used in these experiments were not athermally packaged, nor was the laboratory temperature closely monitored or controlled. Despite these limitations, the system performed adequately, although we might expect that filter drift will be a more significant problem for narrower spectral filters and smaller RF frequencies.

7. Conclusion

We have presented the theory for, and experimentally demonstrated, a new phase-modulated fiber link to simultaneously downconvert and linearize a K-band microwave signal to a VHF IF with improved SFDR. The link does not require a separate optical LO, which greatly simplifies and can improve the reliability of the receiver in comparison with optical heterodyne approaches. Moreover, the system uses only phase modulators that do not require active bias control in the transmitter or receiver. The optical receiver only requires enough bandwidth to cover the IF range, which significantly lowers the component cost of the link in comparison with systems that utilize electrical downconversion. This design is especially amenable to higher frequency links, where downconversion is essential, and optical filtering can be applied to isolate modulation sidebands.

References

[1] A. Seeds, "Microwave photonics," *IEEE Trans. Microw. Theory Tech.*, vol. 50, no. 3, pp. 877–887, Mar. 2002.

[2] C. H. Cox, *Analog Optical Links: Theory and Practice*. Cambridge, U.K.: Cambridge Univ. Press, 2004.

[3] J. Capmany and D. Novak, "Microwave photonics combines two worlds," *Nat. Photon.*, vol. 1, no. 6, pp. 319–330, Jun. 2007.

[4] J.-P. Yao, "Microwave photonics," *J. Lightw. Technol.*, vol. 27, no. 3, pp. 314–335, Feb. 2009.

[5] S. R. O'Connor, M. L. Dennis, and T. R. Clark, "Optimal biasing of a self-homodyne optically coherent RF receiver," *IEEE Photon. J.*, vol. 2, no. 1, pp. 1–7, Feb. 2010.

[6] A. Ramaswamy, L. Johansson, J. Klamkin, H.-F. Chou, C. Sheldon, M. Rodwell, L. Coldren, and J. Bowers, "Integrated coherent receivers for high-linearity microwave photonic links," *J. Lightw. Technol.*, vol. 26, no. 1, pp. 209–216, Jan. 2008.

[7] D. Zibar, L. A. Johansson, H.-F. Chou, A. Ramaswamy, M. Rodwell, and J. E. Bowers, "Novel optical phase demodulator based on a sampling phase-locked loop," *IEEE Photon. Technol. Lett.*, vol. 19, no. 9, pp. 686–688, May 2007.

[8] V. Urick, F. Bucholtz, P. Devgan, J. McKinney, and K. Williams, "Phase modulation with interferometric detection as an alternative to intensity modulation with direct detection for analog-photonic links," *IEEE Trans. Microw. Theory Tech.*, vol. 55, no. 9, pp. 1978–1985, Sep. 2007.

[9] B. Haas, V. Urick, J. McKinney, and T. Murphy, "Dual-wavelength linearization of optically phase-modulated analog microwave signals," *J. Lightw. Technol.*, vol. 26, no. 15, pp. 2748–2753, Aug. 2008.

[10] L. Johansson, H.-F. Chou, A. Ramaswamy, J. Klamkin, L. Coldren, M. Rodwell, and J. Bowers, "Coherent optical receiver for linear optical phase demodulation," in *Proc. IEEE/MTT-S Int. Microw. Symp.*, 2007, pp. 47–50.

[11] T. R. Clark and M. L. Dennis, "Linear microwave downconverting RF-to-bits link," in *Proc. Int. Top. Meeting MWP*, 2008, pp. 12–14.

[12] A. Lindsay, G. Knight, and S. Winnall, "Photonic mixers for wide bandwidth RF receiver applications," *IEEE Trans. Microw. Theory Tech.*, vol. 43, no. 9, pp. 2311–2317, Sep. 1995.

[13] K. Williams and R. Esman, "Optically amplified downconverting link with shot-noise-limited performance," *IEEE Photon. Technol. Lett.*, vol. 8, no. 1, pp. 148–150, Jan. 1996.

[14] G. K. Gopalakrishnan, W. K. Burns, and C. H. Bulmer, "Microwave-optical mixing in $LiNbO_3$ modulators," *IEEE Trans. Microw. Theory Tech.*, vol. 41, no. 12, pp. 2383–2391, Dec. 1993.

[15] G. K. Gopalakrishnan, R. P. Moeller, M. M. Howerton, W. K. Burns, K. J. Williams, and R. D. Esman, "A low-loss downconverting analog fiber-optic link," *IEEE Trans. Microw. Theory Tech.*, vol. 43, no. 9, pp. 2318–2323, Sep. 1995.

[16] C. Sun, R. Orazi, S. Pappert, and W. Burns, "A photonic-link millimeter-wave mixer using cascaded optical modulators and harmonic carrier generation," *IEEE Photon. Technol. Lett.*, vol. 8, no. 9, pp. 1166–1168, Sep. 1996.

[17] K.-P. Ho, S.-K. Liaw, and C. Lin, "Efficient photonic mixer with frequency doubling," *IEEE Photon. Technol. Lett.*, vol. 9, no. 4, pp. 511–513, Apr. 1997.
[18] A. Karim and J. Devenport, "High dynamic range microwave photonic links for RF signal transport and RF-IF conversion," *J. Lightw. Technol.*, vol. 26, no. 15, pp. 2718–2724, Aug. 2008.
[19] M. Howerton, R. Moeller, G. Gopalakrishnan, and W. Burns, "Low-biased fiber-optic link for microwave down-conversion," *IEEE Photon. Technol. Lett.*, vol. 8, no. 12, pp. 1692–1694, Dec. 1996.
[20] R. Helkey, J. Twichell, and C. Cox, "A down-conversion optical link with RF gain," *J. Lightw. Technol.*, vol. 15, no. 6, pp. 956–961, Jun. 1997.
[21] F. Zeng and J. Yao, "All-optical microwave mixing and bandpass filtering in a radio-over-fiber link," *IEEE Photon. Technol. Lett.*, vol. 17, no. 4, pp. 899–901, Apr. 2005.
[22] J. Yao, G. Maury, Y. L. Guennec, and B. Cabon, "All-optical subcarrier frequency conversion using an electrooptic phase modulator," *IEEE Photon. Technol. Lett.*, vol. 17, no. 11, pp. 2427–2429, Nov. 2005.
[23] L. M. Johnson and H. V. Roussell, "Reduction of intermodulation distortion in interferometric optical modulators," *Opt. Lett.*, vol. 13, no. 10, pp. 928–930, Oct. 1988.
[24] L. M. Johnson and H. V. Roussell, "Linearization of an interferometric modulator at microwave frequencies by polarization mixing," *IEEE Photon. Technol. Lett.*, vol. 2, no. 11, pp. 810–811, Nov. 1990.
[25] E. Ackerman, "Broad-band linearization of a Mach–Zehnder electrooptic modulator," *IEEE Trans. Microw. Theory Tech.*, vol. 47, no. 12, pp. 2271–2279, Dec. 1999.
[26] B. M. Haas and T. E. Murphy, "A simple, linearized, phase-modulated analog optical transmission system," *IEEE Photon. Technol. Lett.*, vol. 19, no. 10, pp. 729–731, May 2007.
[27] B. Masella, B. Hraimel, and X. Zhang, "Enhanced spurious-free dynamic range using mixed polarization in optical single sideband Mach–Zehnder modulator," *J. Lightw. Technol.*, vol. 27, no. 15, pp. 3034–3041, Aug. 2009.